

# MODELING OF THE EARTH'S MAGNETIC FIELD AND ITS VARIATIONS WITH ØRSTED, CHAMP, AND ØRSTED-2/SAC-C: CURRENT STATUS AND FUTURE PROSPECTS

Organized by N. Olsen<sup>1</sup>  
 Report by M. Purucker<sup>2</sup>

With contributions from J. Bloxham, C. Constable, H. Kim, S. Maus, M. Manda, N. Olsen, M. Purucker, M. Rother, T. Sabaka, L. Toffner-Clausen, S. Vennerstrøm, and R. von Frese

<sup>1</sup> Danish Space Research Institute, Copenhagen, Denmark, Email: nio@dsri.

<sup>2</sup> Raytheon ITSS at Geodynamics Branch, Goddard Space Flight Center, Greenbelt, MD 20771 USA, Email: purucker@geomag.gsfc.nasa.gov.

## ABSTRACT

A two-day workshop, held September 26-27, 2002 in Copenhagen following the OIST-4 meeting, focused on modeling of the Earth's magnetic field and its variations. Several major themes were covered: 1) Extraction of the Lithospheric Signal, 2) Ionospheric Contributions, 3) Ørsted and CHAMP data center activities 4) Calibration and alignment of magnetic satellite data, 5) Core field and secular variation, 6) the utility and availability of the Comprehensive Magnetic Field Model, and 7) new analysis of old satellite data. Short presentations and discussion followed tutorials. More than 30 scientists and students attended and participated in this very successful workshop,

## INTRODUCTION

Focusing on the modeling of high-precision, multi-spacecraft data, this workshop reported on advances in modeling, and separating, the multitude of magnetic fields encountered in near-earth space.

### EXTRACTION OF THE LITHOSPHERIC SIGNAL

#### Modeling of lithospheric fields (M. Purucker/NASA)

The recent book by Langel and Hinze (1998) provides a summary of modeling methods and is recommended reading. The most used techniques today are spherical harmonic analysis and equivalent source dipoles.

Both techniques need regularization; the process of generating models that puts the least amount of spurious detail into the field. Tables 1 and 2 here give some further details of these techniques.

Several outstanding problems present opportunities for students. First, the amount of new high-quality data generated by the three satellites quickly

overwhelms most modeling techniques. Data by parameter methods are less susceptible to this problem than data by data methods.

### Current Modeling Techniques

Input	Assumption	Output	Name	Variants
$\Delta F$ , and/or components	Truncation at degree $m$ (except for approaches utilizing geomagnetic norms and generalized inverse methods)	$(m+2)$ times $m$ coefficients	Spherical Harmonic Analysis	1) spherical cap 2) two dimensional variants 3) internal external separation 4) non-potential representations
$\Delta F$ , and/or components	Location of basis often specified. Directions (parallel to B) often specified.	6 parameters per dipole, 3 for location, 3 for mag.	Equivalent Source	1) two or three dimensions 2) internal external separation

Table 1

You probably want to consider some simple steps to minimize the data you use, while maximizing the information in that data. For example, don't ask a global basis to do a local job. Use something like collocation with suitably chosen covariances first to reduce the data to a manageable amount, then use spherical harmonics or the equivalent source technique with a global basis.

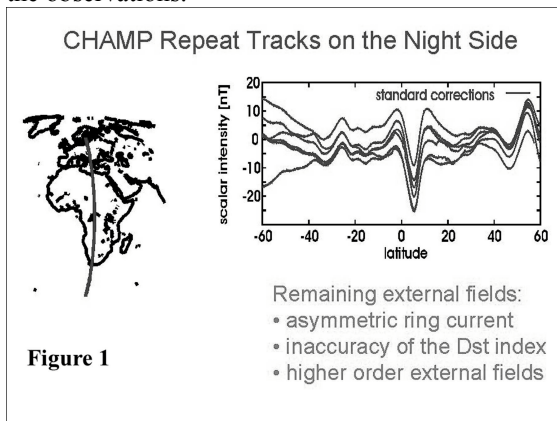
### Current Modeling Techniques

Dealing with instability	Implementation	Who does it?	Name	Reference
Least squares (data by parameter) Robust estimation, magnetic norms and generalized inverse methods (data by data)	Matlab C Fortran	Olsen (DSRI)	Spherical Harmonic Analysis	Langel and Hinze, 1998
		Sabaka (NASA)		Olsen, 2002, GJI
		Constable (Scripps)		
Least squares, Conjugate gradient and sparse matrices, ridge regression	Matlab C Fortran.	Purucker (NASA)	Equivalent Source	Langel and Hinze, 1998
		Ravat		
		Von Frese		

Table 2

Isolating crustal anomalies and other smaller scale features from satellite magnetic data: advantages and drawbacks of along-track filtering, cross-correlation, and line-leveling techniques (S. Maus/GFZ)

This talk focused on the development of physically motivated filters. It began by illustrating, with an example from the CHAMP data, the external fields, which remain even after a field model with internal and external components has been removed from the observations.



How should the remaining external field signal (Figure 1) in these passes over Bangui, the largest crustal anomaly on the Earth, be removed? The following approaches have been tried:

Removing remaining external signal	
• Ad hoc trend corrections	
– linear, parabolic	
• High pass filtering	
– Kaiser filter, Butterworth filter	
• Fit and remove a polynomial	
• Correlation analysis	
• Cross-over analysis	

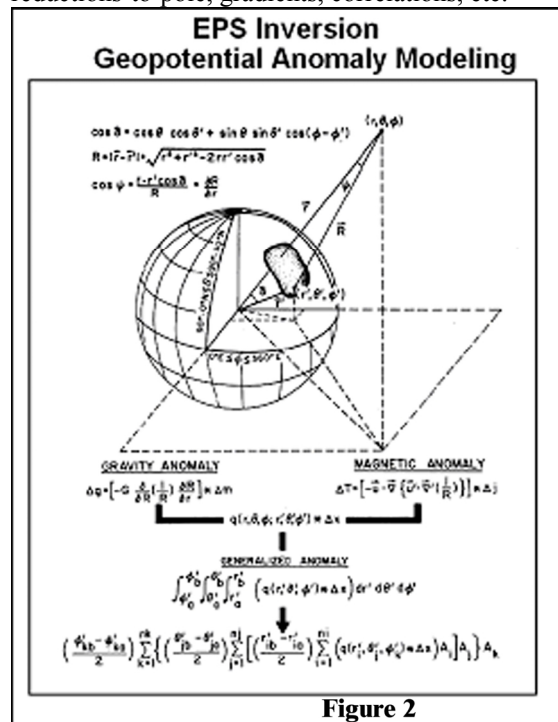
**Table 3**

This was followed by the definition of a suitable, physically motivated polynomial. It was shown that the removal of such a polynomial removed little crustal anomaly or small-scale signal.

The discussion by R. Haagmans (ESA) raised the possibility of using spherical harmonic filters (Haagmans, 2000; Jakob-Chien and Alpert, 1997).

## Satellite magnetic anomalies for lithospheric exploration (R. von Frese and H. Kim/OSU)

The magnetic workshop considered two contrasting perspectives for processing satellite magnetic observations for lithospheric anomalies. The typical global geophysics approach represents and analyzes satellite magnetic data by spherical harmonics that emphasize the more regional anomaly attributes for lithospheric analysis. However, a fuller exploitation of the local anomaly details in the track coverage is possible from the exploration geophysics approach that uses spherical coordinate distributions of equivalent point sources (EPS) to model and analyze the satellite magnetic observations. Indeed, any local-through-global distribution of satellite magnetic data may be related to the effects of point dipole arrays by EPS inversion (Figure 2) for estimating spherical coordinate anomaly continuations, interpolations, differential reductions-to-pole, gradients, correlations, etc.



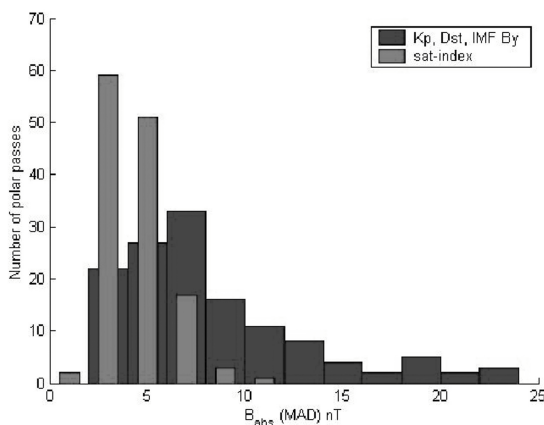
Furthermore, adapting equivalent point sources for Gauss-Legendre quadrature integration (Figure 2) is very effective for relating satellite magnetic anomalies to arbitrary spherical coordinate distributions of lithospheric magnetizations. These two perspectives, in principle, should produce complimentary results at Both local and global scales. In practice, however, lithospheric studies tend to focus on more local (i.e. spherical patch) distributions of satellite magnetic observations where the exploration geophysics approach clearly offers significant advantages. This presentation is fully developed in these proceedings in a paper by von Frese and Kim entitled "Satel

Its magnetic anomalies for lithospheric exploration”.

*IONOSPHERIC CONTRIBUTIONS*

**Ionospheric contributions to satellite based internal field modeling: New selection criteria? (S. Vennerstrøm, DSRI)**

Contamination of internal field models by high-latitude ionospheric currents was discussed. At present, this contamination is being minimized in the global modeling by data selection, using only quiet intervals in the modeling. The data-selection is based mainly on the low-latitude indices Kp and Dst, which have the advantage of being available with a very short time-delay. It was however demonstrated that intervals that meet the currently used selection criteria can be very disturbed in the polar regions as measured by the mean average deviation from the internal field model of the absolute magnitude of the field Babs(MAD) measured by CHAMP or Ørsted. The question of whether the satellite data could be used as an alternative in the data selection process was then examined. The basic idea was that the presence of ionospheric currents could be detected in the magnetic field component perpendicular to the internal field. This component does not enter most of the present models, which over the polar regions only uses the absolute measurements. Due to the relative size of the internal and external magnetic fields the perpendicular component has no measurable effect on the absolute value of the measured field. Using the average size of the perpendicular component over the polar regions to select the quiet intervals would therefore be a selection procedure based on the part of the satellite data, which do not otherwise enter the modeling. The relationship between the average perpendicular component and Babs(MAD) was investigated statistically, and these were shown to be highly related. It was shown that a selection procedure based on the average perpendicular component was superior to the current methods in terms of



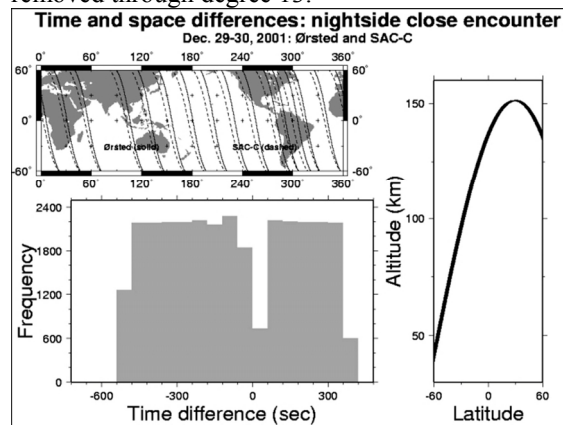
minimizing Babs(MAD).

Figure caption: Histograms of Babs(MAD) measured by CHAMP for a selection of quiet intervals based on current methods (Kp, Dst, IMF By) compared to a selection based on the average perpendicular component over the polar regions. Both selections were made for the same time-interval: autumn 2001. The threshold value of the average perpendicular component was adjusted so that the same percentage of data was selected in the two cases.

*CALIBRATION AND ALIGNMENT OF MAGNETIC SATELLITE DATA*

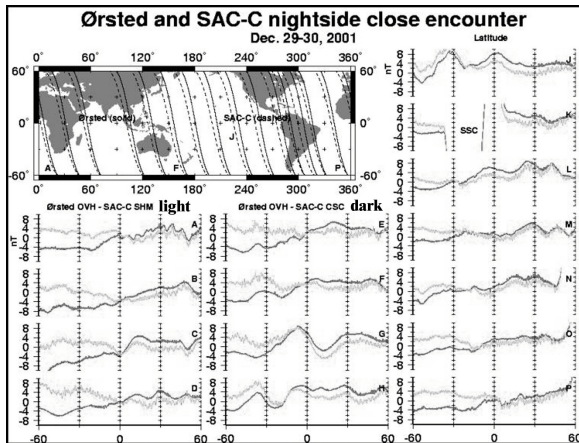
**Intercalibration of the scalar and vector magnetometers on SAC-C with those on CHAMP and Ørsted (M. Purucker/NASA)**

The scalar (SHM) and vector (CSC) magnetometers on SAC-C are undergoing calibration. As part of this process, the SAC-C magnetometer outputs were compared to their counterparts on CHAMP and Ørsted during close encounters of the satellites. The premise is that during close encounters, the ionospheric and magnetospheric fields seen by the spacecraft will be similar. Three close encounters were selected: 21 May 2001, 29 December 2001, and 15 June 2002. The December and June close encounters were co-rotating encounters; during the May encounter the satellites were counter-rotating. The May and June close encounters occurred on magnetically quiet days while the December encounter occurred in the midst of an active geomagnetic period, with an SSC occurring in the middle of the encounter. The analysis was preceded by the removal of a main field model (internal components only). For the May and June encounters the IDEMM model (Olsen et al, 2002) was removed through degree 46 while for the December encounter the 10b/01 field model was removed through degree 13.



The figure above shows both the time and space differences associated with the nightside close encounters of the Ørsted and SAC-C in late December 2001. The time difference, in seconds, is measured as the time between identical latitude crossings.

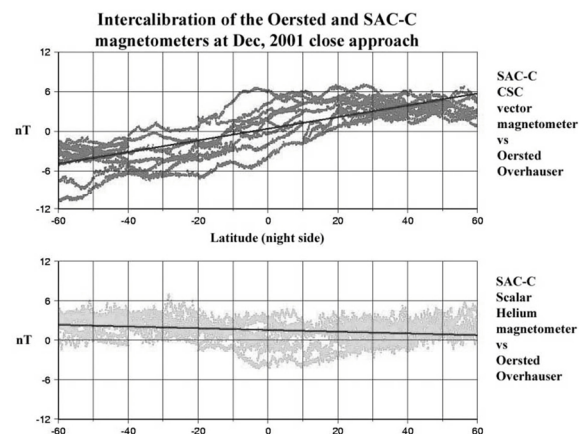
One component of the space difference, the altitude, is also shown. This is also measured at the same latitude. The longitude differences are shown on the global map, and vary from no separation at 60 degrees South to about five degrees separation at 60 North latitude.



After removal of the main field model through degree 13, the SAC-C data was resampled at the Ørsted latitude locations. The difference between the Ørsted and SAC-C residuals is a measure of the changes necessary to bring the SAC-C vector and scalar magnetometers into agreement with the absolute Ørsted Overhauser (OVH) magnetometer.

This approach fails in situations where the internal magnetic field from the lithosphere or ionosphere varies significantly on spatial scales comparable to the longitudinal separation of the two spacecraft. This failure has a diagnostic signature. Both residuals will co-vary and form a high-low or low-high pair that extends typically across 20 degrees of latitude. Typical examples can be seen on Pass 'G' near the equator and Pass 'H' at about 20 degrees South latitude. Two approaches to dealing with this problem are to remove a high degree static model from the original data or to discard the data in the affected regions (adopted in this presentation).

Note the sudden storm commencement (SSC) evident on Pass 'K' in simultaneous observations



from SAC-C and Ørsted. The SSC is also evident in the simultaneous CHAMP observations. The SSC occurs on 29 Dec 2001 at 05:20 UT.

The corrections necessary to bring the magnetometers into agreement are shown above, based on segments of the residuals from the previous plot. Best fits to the residuals are shown with the dark line. These corrections, at least for the scalar helium magnetometer (SHM), have been confirmed by comparison with a CHAMP close encounter and an encounter where the SAC-C spacecraft is traveling in the opposite direction.

Further details on this close encounter, and other close encounters, can be found at [www.dsri.dk/multimagatellites/types/calibration.html](http://www.dsri.dk/multimagatellites/types/calibration.html).

ØRSTED AND CHAMP DATA CENTERS

Current status of Ørsted and Ørsted-2 Data Processing (L. Toffner-Clausen/DMI)

Ørsted data – Outstanding issues

The Ørsted data are now being processed to a level (2.4) of accuracy, which is believed to be very close to the final level. Small adjustments to the applied calibrations and corrections may still be made, e.g. to the corrections of the ACS magnetorquer-coils disturbances. These disturbances are however very small-less than 1.3 nT for more than 99% of the mission, and the remaining error after the current correction is expected to be less than 0.5 nT for all times

The method to smooth and interpolate attitude data (SIM data) produce one-second attitude information is still being investigated. We hope to have a solution soon. We also need to finalize the processing of the two indicators of the magnetic vector measurements:  $B_{AC}$  (5-30 Hz fluctuations) and  $B_{\sigma}$  (error estimates). And we plan to produce a boom oscillation indicator indicating the amplitude of boom oscillations in the range around 0.3 to 0.5 Hz. When this is ready, MAG-L data files will be produced in this form.

Ørsted-2 Data – Current Status

**SHM**-Scalar Helium Magnetometer. NASA/GSFC is investigating.

**CSC**-Vector magnetometer. In-flight calibrations have not yet proven satisfactory. DSRI is investigating.

**IST**-Italian Star Tracker- We have received attitude data from this body-mounted star tracker-imager.

DSRI is investigating the possibilities of using these data.

## Current status of CHAMP Data Processing (M. Rother/GFZ)

Currently the only available CHAMP magnetic field data are corrected and in-flight calibrated field data at Level-2. Both vectors from the fluxgate magnetometer and scalar data from the Overhauser magnetometer are available. The corrections applied to the data are based on ground calibration efforts, sensor sensitivities, misalignments, offsets, static time adjustments, and satellite fields. The scalar calibration using the absolute Overhauser observations is run on a daily basis and the input parameter set for the fluxgate processing is updated every two weeks. Therefore, the amplitude of the scalar residuals between the fluxgate and Overhauser magnetometers will depend on the number of days since the last parameter set update.

Unexplained differences of between 0.11 and 1 nT still remain between the fluxgate and Overhauser magnetometers after all of these standard corrections have been applied. Furthermore, we found that there are two additional parameters to fit: two time shifts seem to be a function of time

- 1) a phase shift between the OVM and FGM sensors, currently between 10 and 20 ms.
- 2) A phase shift of the CSC temperature sensor. We have found on ground calibration a value of about 8 minutes, but this seems to have a wide variability till changing the sign. But most probably we are fitting another, unknown influence with this free parameter.

## Helper script for handling CHAMP-ISDC data

To help people who are downloading magnetic field data from the CHAMP-ISDC there is a simple perl script available which can be run on Linux boxes. This script can initiate the batch-mode without using a browser, and will try to download the requested files from the ISDC download area and clean the download area for the next try. A valid password for public access to the ISDC is still required, but the script can simplify the process. For more information use the help text of the script itself. It is called `getisdc.pl` and can be found at: [www.gfz-potsdam.de/pb2/pb23/SatMag/suppl.html](http://www.gfz-potsdam.de/pb2/pb23/SatMag/suppl.html)

### *CORE FIELD AND SECULAR VARIATION*

## Geodynamo Modelling and Geomagnetic Field Modelling: A two-way street (J. Bloxham/Harvard)

At present, most of the 'traffic' is from geomagnetic field modeling to geodynamo modeling. In other words, data and field models are far more important for geodynamo modeling than geodynamo modeling is for geomagnetic field modeling. What is needed is an entirely new approach. Current methods are based on the extrapolation of observations. What is needed is to use techniques of data assimilation, as in weather forecasting.

As part of this shift, two presently separate fields, field modeling and dynamo modeling, need to merge. Data assimilation is highly developed in the meteorological and oceanographic community. The observations for such assimilation don't need to be of the variables computed in the model. They only need to be linear functions of the variables.

### Geomagnetic field modelling $\rightleftharpoons$ geodynamo modelling

- Dynamical regime of the core
  - Steady/slowly-varying background flow
    - \* tangentially-geostrophic near core surface
    - \* associate with magnetostrophic zeroth order balance in core
    - \* what is the timescale of this flow?
    - \* how much is it influenced by core-mantle interaction?
  - Superimposed field of torsional oscillations
    - \* evidence from core angular momentum calculations
    - \* fits of toroidal oscillations to time-dependent flow calculations
    - \* provides an explanation for geomagnetic jerks

## A compilation of existing geomagnetic field models, external field models, and a bibliography (M. Manda/IPGP)

Attached to the back of this workshop report is an up-to-date compilation of existing field models, courtesy of M. Manda and her students.

## THE UTILITY AND AVAILABILITY OF THE COMPREHENSIVE MAGNETIC FIELD MODEL (CM): THE CM USER GROUP

An introduction by D. Ravat was followed by a presentation from T. Sabaka. Participants suggested enhancements to the CM, which would make it more valuable to them. The following enhancements have now been added by Sabaka and Olsen: 1) output is now available either in the space or frequency domain (as spherical harmonic coefficients), 2) External fields can now be output as a current (**J**), 3) magnetic indices (Dst, F10.7) can be automatically selected, 4) availability of observatory biases, which are now appended to the spherical harmonic model coefficient file, and 5) development of an official Web page for dissemination of information and communication with the user community.

## Comprehensive magnetic field modeling: Two applications (C. Constable, Scripps)

C. Constable discussed the application of the Comprehensive field model (Sabaka et al, 2002) to 1) isolating the crustal contribution to the field and using this to find the Lowes-Mauersberger spectrum (Korte et al., 2002), and 2) isolating the large-scale magnetospheric contributions for Earth induction studies.

### *NEW ANALYSIS OF OLD SATELLITE DATA (A.Jackson/Leeds)*

A tutorial by A. Jackson followed by a discussion. This presentation appears as a short paper in these proceedings by Jackson and Olsen entitled 'Possibilities for Re-analysis of Old Satellite Data'.

### *SUMMARY*

The informal talks discussed here resulted in a fruitful exchange of ideas. We hope it was especially helpful for students.

### *ACKNOWLEDGMENTS*

We want to thank the Ørsted, Ørsted-2/SAC-C, and CHAMP projects for their support.

### *SUGGESTIONS FOR FURTHER READING AND REFERENCES*

Korte, M., C. Constable, and R. Parker (2002), Revised magnetic power spectrum of the oceanic crust, *J Geophys. Res.*, 107(B9), 2205, doi:10.1029/2001JB001389.

Haagmans, R., (2000), A synthetic earth for use in geodesy, *J. of Geodesy*, v. 74, pp. 503-511.

Jakob-Chien, R., and B. Alpert, (1997), A fast spherical filter with uniform resolution, *J. of Computational Physics*, v. 136, pp. 580-584.

Langel, R.A. and W. J. Hinze, (1998), *The magnetic field of the Earth's lithosphere: The satellite perspective*, Cambridge, 429 pp.

Olsen, N. (2002), A model of the geomagnetic field and its secular variation for epoch 2000 estimated from Ørsted data, *Geophys. J. Int.*, v. 149, pp. 454-462.

Olsen, N., R. Holme, and H. Lühr, (2002), A magnetic field model derived from Ørsted, CHAMP, and Ørsted-2/SAC-C observations, *Eos. Trans. AGU*, 83(19), *Spring meet. Suppl.*, Abstract GP21A-01. Available online at [www.dsri.dk/multimagsatellites](http://www.dsri.dk/multimagsatellites)

Sabaka, T., N. Olsen., and R. Langel, (2002): A comprehensive model of the quiet-time, near-Earth, magnetic field: Phase 3, *Geophys. J. Int.*, Vol. 151, pp. 32-68.

Geomagnetic field models

Model	Period – data	MF, SV degree / order	Time (LT)	Kp	Dst	Another index / criteria	Geomagnetic latitude	Uniformity	Observations
CO2: Holme, Olsen, Rother, Lühr	<ul style="list-style-type: none"> <li>● Champ, Ørsted, Ørsted-2/SAC-C</li> <li>● obs.</li> </ul>	MF: 29 SV: 13 EXT: 2	18:00-06:00 LT	Kp ≤ 1 (data) Kp ≤ 2o (3 hr*)	Dst  ≤ 10 nT  d(Dst)/dt  < 3 nT/hr	By  > 3 nT (too strong dawn-dusk IMF component eliminated)	<ul style="list-style-type: none"> <li>● vector : lat. ≤ 50°</li> <li>● scalar : lat. &gt; 50° or if altitude data not available</li> </ul>	Non-Gaussian distribution: IRLS (iteratively reweighted least squares), Huber weights	CHAMP: lower altitude = better sensitivity to high degree n coefficients
CM3: Sabaka, Olsen, Langel (Geophys. J. Int.)	<ul style="list-style-type: none"> <li>● Magsat</li> <li>● obs.: OHM-1am (4 hr*) OHM-MUL (1 quiet day/month)</li> </ul>	MF: 65 SV: 13	Non-LT terms	Kp ≤ 1- (data) Kp ≤ 2o (3 hr*) (Magsat)	-20 ≤ Dst ≤ 50 nT (Magsat)	F10.7: solar radiation flux index; 1 value / yr, corrected for : <ul style="list-style-type: none"> <li>● uncertainty of the antenna gains</li> <li>● Earth reflected waves</li> </ul>	<ul style="list-style-type: none"> <li>● vector : lat. ≤ 50°</li> <li>● scalar : all lat.</li> </ul>	<ul style="list-style-type: none"> <li>● time: Magsat data nov-dec 1979, jan-feb 1980, mar-apr 1980</li> <li>● space: satellite passes added for sparse regions</li> </ul>	Weighting hypothesis: <ul style="list-style-type: none"> <li>● lat ≤ 50°: OHM-1H &amp; OHM-MUL &amp; Magsat dawn and dusk are isotropic processes</li> <li>● lat &gt; 50°: OHM-MUL &amp; Magsat dawn and dusk processes are isotropic in the XY plane</li> </ul>
IGRF 2000 Olsen, Sabaka, Tøffner-Clausen (EPS, 2000)	<ul style="list-style-type: none"> <li>● Ørsted:</li> <li><b>a</b> - may 1999</li> <li><b>b</b> - sep 1999</li> <li><b>c</b> - mar-sep 99 (scalar)</li> <li>- may-sep 99 (vect.)</li> </ul>	MF: 12	night side	Kp ≤ 1+ (3 hr) Kp ≤ 2o (3 hr*)	Dst ignored (± 20nT)	external field contributions: selection according to Kp	vector: lat. < 50°	<ul style="list-style-type: none"> <li>● declination for scalar and vector data: times of measurement &gt; 30 sec apart</li> <li>● weighting: equal area simulation</li> </ul>	<ul style="list-style-type: none"> <li>● noise reduction in the rotation angle of the star imager</li> </ul>
IGRF 2000 Maemillan, Quinn (EPS, 2000)	<ul style="list-style-type: none"> <li>● Ørsted</li> <li>● obs.: 190</li> <li>● repeat stations</li> </ul>	MF: 12 SV: 8 EXT: 5	0 - 2 am LT	Kp ≤ 2+	Dst  ≤ 30 nT	<ul style="list-style-type: none"> <li>● residuals &lt; 1000 nT with respect to 1995.0</li> </ul>	<ul style="list-style-type: none"> <li>● vector : lat. &lt; 50°</li> <li>● long.: 5° (eq.) - 120° (poles)</li> <li>● 10°x10°: only sat. data</li> <li>● declination: every 20<sup>th</sup> sample chosen = every 20<sup>th</sup> sec</li> </ul>	<ul style="list-style-type: none"> <li>● weighted outliers</li> </ul>	
IGRF 2000 Langlais, Mandea (EPS, 2000)	<ul style="list-style-type: none"> <li>● main field:</li> <li>- sat., obs. (vector)</li> <li>- marine (scalar)</li> <li>● SV: monthly means</li> </ul>	MF: 10 SV: 8	● local night time (MF)	Kp ≤ 2o (MF, scalar marine)	Dst  ≤ 10 nT	<ul style="list-style-type: none"> <li>● MF: residuals &lt; 500 nT with respect to 1997.5 model</li> </ul>	<ul style="list-style-type: none"> <li>● north going orbits chosen</li> <li>● equal-area simulation (see declination)</li> <li>● weighting: w = 1 (0:00 MLT) w ~ max (cos(T/2), 0) T = local time (rad) Σw = 13 (UT = 8:00) Σw = 48.7 (UT = 20:00)</li> </ul>	<ul style="list-style-type: none"> <li>● extrapolation of some monthly means</li> <li>● geographical weights</li> </ul>	
Olsen (Geophys. J. Int., 2002)	<ul style="list-style-type: none"> <li>● Ørsted</li> <li>● obs. mar 1999 - sep 2001</li> </ul>	MF: 29 SV: 13	● local night time (sat. & obs.)	Kp ≤ 1+ (data) Kp ≤ 2o (3 hr*)	d(Dst)/dt  ≤ 3 nT/hr	<ul style="list-style-type: none"> <li>● RC: hourly means -&gt; linear slope -&gt; subtraction from each component at each observatory.</li> <li>● Each hr: dP<sup>o</sup>/dθ<sub>obs</sub> = - sinθ<sub>obs</sub> is fitted to ΔX<sub>obs</sub> (residual in the direction of N mag. pole).</li> <li>● RC = amplitude of this term</li> <li>● polar caps: data rejected if  By  &gt; 3 nT</li> </ul>	lat. ≤ 60° (for RC criterion) vector : lat. ≤ 50° scalar : lat. > 50°	<ul style="list-style-type: none"> <li>● 145 obs.</li> <li>● 93 observations: 1980-1998</li> <li>● 67 repeat stations</li> </ul>	<ul style="list-style-type: none"> <li>● correction for the local time drift of the Ørsted orbit plane</li> <li>● declination: at least 60 sec / sinθ</li> <li>● θ = geogr. colatitude</li> <li>● recalibration &amp; correction for stellar aberration</li> </ul>
Olsen (2002, nio_RC.html)	<ul style="list-style-type: none"> <li>● 1 sep - 31 dec 2001 (Champ, Ørsted, Ørsted-2/SAC-C)</li> <li>● 1998 - 2000 (obs.)</li> </ul>		18:00-06:00 MLT (model subtracted from the data)			<ul style="list-style-type: none"> <li>● RC from obs. &amp; sat. scalar residuals</li> <li>● 5 day running mean RC = - q<sub>1</sub><sup>0</sup></li> </ul>	lat. ≤ 60° (sat. & obs.)	<ul style="list-style-type: none"> <li>● weighting: w = 1 = max (obs., 0 MLT) w = min (dawn, dusk)</li> <li>● w decreases cf. max (cos(T/2), 0) T = LT (radians)</li> </ul>	<ul style="list-style-type: none"> <li>● 8 Gauss coefficients estimated with IRLS &amp; Huber weights</li> <li>● RC: better for the quiet-time contribution than the (previsional) Dst index</li> </ul>
Langlais, Mandea, Utré-Guéraud (PEPI, 2002)	<ul style="list-style-type: none"> <li>● Magsat: 1979-1980, 7 months</li> <li>● Ørsted:</li> <li>mar. 1999 - apr. 2000</li> </ul>	MF: 29 EXT: 2 SV: 13	<ul style="list-style-type: none"> <li>● Magsat: dawn-side</li> <li>● Ørsted: night-time (equator: 3 - 8 pm LT)</li> </ul>	Kp ≤ 1+ (data) Kp ≤ 2- (3 hr*)	Dst  ≤ 5 nT  d(Dst)/dt  ≤ 3 nT/hr		scalar: lat. > 50°	<ul style="list-style-type: none"> <li>● Ørsted: anisotropic weights: - uncertainty in the attitude - rotation of the camera</li> <li>● MAGSAT: isotropic weights</li> </ul>	<ul style="list-style-type: none"> <li>● comparison with predicted values</li> <li>● outliers removed</li> </ul>
<i>Comparison between IGRF 2000 models</i>									
Mandea, Langlais (EPS, 2000)	Ørsted		night side 3 hr intervals	Kp = 0o or Kp = 0+				2 sets: 10 points / (5°x5°) 10 points / (10°x10°)	<ul style="list-style-type: none"> <li>● in-flight calibration correction</li> </ul>

Abbreviations: obs. = observatories, sat. = observatories, LT = local time, hr\* = hours before the measurement moment, MF = main field, SV = secular variation, EXT = external component

## Bibliography

- Holme, R., N. Olsen, M. Rother, H. Lühr, CO2: A CHAMP magnetic model.  
 Sabaka, T.J., N. Olsen, R.A. Langel, A Comprehensive Model of the Quiet-Time, Near-Earth Magnetic Field: Phase 3. *Geophys. J. Int.*  
 Olsen, N., A model of the geomagnetic field and its secular variation for epoch 2000 estimated for Ørsted data. *Geophys. J. Int.*, **149**, pp. 454-462, 2002.  
 Langlais, B., M. Mandea, An IGRF candidate main geomagnetic field model for epoch 2000 and a secular variation model for 2000-2005. *Earth Planets Space*, **52**, pp. 1137-1148, 2000.  
 Mandea, M., B. Langlais, Use of Ørsted scalar data in evaluating the pre-Ørsted main field candidate models for the IGRF 2000. *Earth Planets Space*, **52**, pp. 1167-1170, 2000.  
 Macmillan, S., J.M. Quinn, The 2000 revision of the joint UK/US geomagnetic field models and an IGRF 2000 candidate model. *Earth Planets Space*, **52**, pp. 1149-1162, 2000.  
 Olsen, N., T.J. Sabaka, L. Tøffner-Clausen, Determination of the IGRF 2000 model. *Earth Planets Space*, **52**, pp. 1175-1182, 2000.  
 Olsen, N, Comparison between Dst and RC. Monitoring Magnetospheric Contributions using Data from Ørsted. *Champ and Ørsted-2/SAC-C<sub>2</sub>*, 2002. [http://www.dsti.dk/multimagatellites/virtual\\_talks/olsen/noi\\_RC.html](http://www.dsti.dk/multimagatellites/virtual_talks/olsen/noi_RC.html).  
 Langlais, B., M. Mandea, P. Ulrich-Guérard, High-resolution magnetic field modeling: application to MAGSAT and Ørsted data. *P.E.P.I.*, accepted, 2002.

### External field models

Model	Period – data	MF, SV degree / order	Time (LT)	Kp	Dst	Another index / criteria	Geomagnetic latitude	Uniformity	Observations
Tsyganenko external field model (1996)					-100 ≤ Dst ≤ 20 nT	Does not include AE as input parameter $0.5 \leq P_{sw} \leq 10$ nPa (solar wind pressure) $-10 \leq B_{y_{IMF}}, B_{z_{IMF}} \leq 10$ nT			

### External field models and their parameters

Description	Field model		Default value	Minimum value	Maximum value
Kp	Mead-Fairfield, Tsy87s, Tsy87l, Tsy89, Ostapenko-Maltsev		0	0	9
Dst (nT)	Olson-Pfizer dynamic, Tsy96, Ostapenko-Maltsev		-30	-600	50
Solar wind pressure (nPa)	Tsy96, Ostapenko-Maltsev		3	0.5	10
Solar wind density (cm <sup>-3</sup> )	Olson-Pfizer dynamic		25	1	100
Solar wind velocity (km s <sup>-1</sup> )	Olson-Pfizer dynamic		300	100	1200
$B_{IMFz}$ (nT)	Tsy96		0	-50	50
$B_{IMFz}$ (nT)	Tsy96, Ostapenko-Maltsev		0	-50	50

## Bibliography

- Bartels, J., The eccentric dipole approximating the Earth's magnetic field, *J. Geophys. Res.*, **41**, pp. 225-250, 1936.  
 Cain, J.C., S.J. Hendricks, R.A. Langel, W.V. Hudson, A proposed model for the international geomagnetic reference field-1965, *J. Geomag. Geoelectr.*, **19**, pp. 335-355, 1967.  
 Fraser-Smith, A.C., Centered and Eccentric Geomagnetic Dipoles and Their Poles, 1600-1985, *Rev. Geophys.*, **25**, 1, pp. 1-16, 1987.  
 Jensen, D.C., J.C. Cain, An interim geomagnetic field, *J. Geophys. Res.*, **67**, pp. 3568, 1962.  
 Olson, W.P., A model of the distributed magnetospheric currents, *J. Geophys. Res.*, **79**, pp. 3731-3738, 1974.  
 Olson, W.P., K.A. Pfizer, Magnetospheric magnetic field modeling, *Annual Scientific Report, AFOSR Contract No. F44620-75-C-0033*, 1977.  
 Ostapenko, A.A., Y.P. Maltsev, Relation of the magnetic field in the magnetosphere to the geomagnetic and solar wind activity, *J. Geophys. Res.*, **102**, pp. 17467-17473, 1997.  
 Peddie, N.W., International Geomagnetic Reference Field: The Third Generation, *J. Geomag. Geoelectr.*, **34**, pp. 309-326, 1985.  
 Pfizer, K.A., W.P. Olson, T. Mogsstad, A time dependent source driven magnetospheric magnetic field model, *EOS*, **69**, pp. 426, 1988.  
 Tsyganenko, N. A., Global quantitative models of the geomagnetic field in the cislunar magnetosphere for different disturbance levels, *Planet. Space Sci.*, **35**, pp. 1347-1358, 1987.

Tsyganenko, N. A., A magnetospheric magnetic field model with a wrapped tail current sheet, *Planet. Space Sci.*, **37**, pp. 5-20, 1989.  
Tsyganenko, N. A., and D. P. Stern, Modeling the global magnetic field the large-scale Birkeland current systems, *J. Geophys. Res.*, **101**, pp. 27187-27198, 1996.  
<http://www.spenvis.oma.be/spenvis/help/models/bkxtra/bkxtrapar.html#TABLE>.